Modeling and Analysis

GREENHOUSE GASES SCIENCE AND TECHNOLOGY

The variation in composition of ultramafic rocks and the effect on their suitability for carbon dioxide sequestration by mineralization following acid leaching

M. T. Styles,* British Geological Survey, Keyworth, Nottingham, UK
A. Sanna, Heriot-Watt University, Edinburgh, UK
A. M. Lacinska and J. Naden, British Geological Survey, Keyworth, Nottingham, UK
M. Maroto-Valer, Heriot-Watt University, Edinburgh, UK

Abstract: Carbon dioxide capture and storage by mineralization has been proposed as a possible technology to contribute to the reduction of global CO_2 levels. A main candidate as a feed material, to supply Mg cations for combination with CO_2 to form carbonate, is the family of ultramafic rocks, Mg-rich silicate rocks with a range of naturally occurring mineralogical compositions. A classification scheme is described and a diagram is proposed to display the full range of both fresh and altered ultramafic rock compositions. This is particularly for the benefit of technologists to raise the awareness of the variation in possible feedstock materials. A systematic set of acid leaching experiments, in the presence of recyclable ammonium bisulphate, has been carried out covering the range of ultramafic rock compositions. The results show that lizardite serpentinite releases the most Mg with 78% removed after 1 h, while an olivine rock (dunite) gave 55% and serpentinized peridotites intermediate values. Antigorite serpentinite only released 40% and pyroxene- and amphibole-rich rocks only 25%, showing they are unsuitable for the acid leaching method used. This wide variation in rock compositions highlights the necessity for accurate mineralogical characterization of potential resources and for technologists to be aware of the impact of feed material variations on process efficiency and development.

Keywords: ultramafic rocks; rock classification; serpentinite; carbon dioxide sequestration by mineralization; acid leaching

Introduction

Carbon dioxide capture and storage by mineralization (CCSM) is a promising technology in the carbon capture and storage (CCS) portfolio to meet the Kyoto target on CO_2 emissions reduction.[1]

The basis of the process is to extract divalent cations (in this case Mg) from a feed material and combine these with CO_2 to form a stable carbonate mineral,

Correspondence to: M. T. Styles, British Geological Survey, Keyworth, Nottingham NG12 5GG, UK. E-mail: mts@bgs.ac.uk
Received December 9, 2013; accepted December 13, 2013
Published online at Wiley Online Library (wileyonlinelibrary.com). DOI: 10.1002/ghg.1405

permanently locking away the CO_2. An example of the type of reaction involved is shown below:

$$4Mg_2SiO_4 + 8CO_2 = 8MgCO_3 + 4SiO_2 \quad (1)$$

Mg-olivine magnesite quartz

The CCSM process will require a large stock of material that can, after appropriate processing, provide a source of cations for combination with CO_2 to form stable carbonate. There are few elements present at or near the Earth's surface in large amounts that are suitable for forming stable (insoluble in water) carbonates; in practice these elements are limited to Mg and Ca. By far the most common Ca-rich rock is limestone, where the Ca is already present as carbonate, and other Ca-rich rocks are rare. Sources from rocks will have to be Mg-rich silicate rocks, known as ultramafic rocks.

Potential global resources of ultramafic rocks are enormous,[2] but recently, it has been estimated that most likely, about one-fifth of the global CO_2 emissions could be targeted by this technology in terms of materials handling.[3] CCSM technology has not yet been deployed due to high energy consumption and costs that are mainly related to the slow dissolution kinetics of Mg extraction from the silicate feed materials.[4–6]

The overall mineral carbonation process requires large amount of chemicals to extract the cations from silicate feedstock. Therefore there is a necessity to develop a process that will not only catalyze the single steps of mineral carbonation but can also recycle the chemicals and potentially lower the overall costs. Recently, mineral carbonation in the presence of ammonium salts has attracted particular attention,[7–11] since the chemicals used can be recycled in the process. It has been estimated that about 11t ammonium bisulphate (95% recyclable) are required to dissolve 4.9t serpentine containing 1.2t of Mg.[7]

Many previous publications covering CCSM refer to ultramafic rocks as if they were a single, homogeneous rock or a limited range of simple compositions,[12,13] but in fact they are a family of rocks with different mineralogical and chemical compositions that has only rarely been mentioned by previous authors.[2] This variation affects their suitability as a feed material for CCSM. The variation and geological classification of ultramafic rocks is well known to geological specialists but here it is described in relatively simple terms, emphasizing the aspects most relevant to CCSM. The classification scheme proposed is intended to be informative for technologists with little geological background. Detailed discussion of the formation and alteration of ultramafic rocks is considered outside the scope of this paper, as only the final mineral composition is of relevance to the CCSM process. The use of specialist geological terms is kept to a minimum.

The capacity to extract Mg from the feed material is a vital property and a high degree of efficiency will be crucial to any industrial scale process involving enormous amounts (gigatonnes) of material. We describe the testing of the range of compositions of ultramafic rocks for suitability for use in a CCSM process based on ammonium salts acid leaching.

Classification of ultramafic rocks

Ultramafic rocks are composed of more than 90% mafic (i.e. dark-colored) minerals in various proportions with trace amounts of other minerals. The main mafic minerals are the Mg-silicates: olivine (Mg_2SiO_4), orthopyroxene ($MgSiO_3$), and clinopyroxene ((MgCa)SiO_3). In most rocks, a proportion of the Mg in the crystal structure of these minerals is substituted by Fe^{2+}. In the rocks considered in this study, maximum substitution is only around 10% and for the sake of simplicity only the names of the mineral or the Mg end-member will be used.

Ultramafic rocks are formed by the crystallization of an anhydrous, Mg-rich silicate melt at temperatures around 1200 °C. This usually occurs in the middle or lower parts of the Earth's crust or in the Earth's mantle. The internationally accepted classification for fresh ultramafic rocks is used in a slightly modified form by the British Geological Survey.[14] This is shown in Fig. 1, with the names used for the rocks and the proportions of the various minerals. The apices of the triangle show rocks composed of 100% of a particular mineral, and the inner parts of the triangle show various proportionate mixtures of the minerals. The Mg and Ca contents of the different minerals are indicated in red and blue, respectively. This indicates that rocks rich in olivine are the best targets as they have the highest divalent cation and the lowest silica content. Rocks consisting dominantly of olivine are known as peridotites, whereas those in which pyroxene is dominant are termed pyroxenites.

After formation of the ultramafic rocks at depth in the Earth, tectonic processes and erosion over millions of years can bring them to the near surface

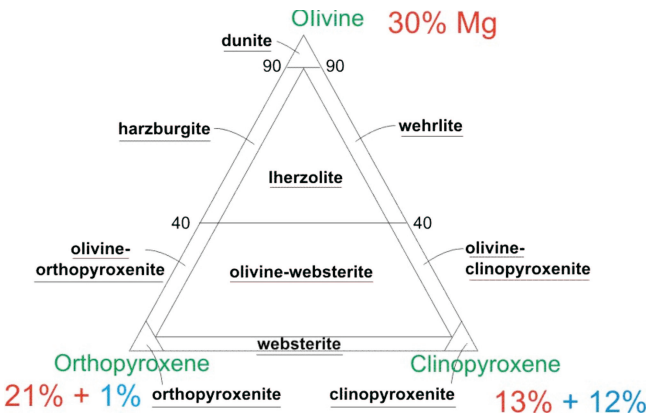

Figure 1. The classification of fresh, anhydrous ultramafic rocks. The Mg content of the rocks at each apex is shown in red and the Ca content in blue (weight% element).

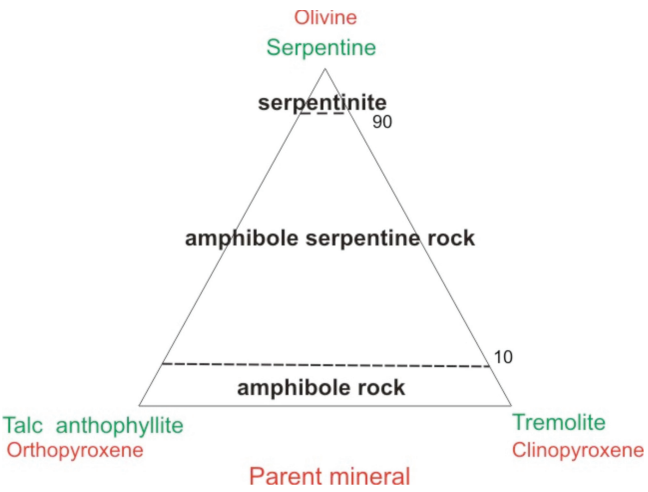

Figure 2. Classification of hydrated ultramafic rocks. The actual minerals present are shown in green and the parent anhydrous minerals in red.

environment where they are now located and potentially available as a source material for CCSM. Rocks that were in equilibrium in an anhydrous, high-temperature environment become highly unstable during this transport to the surface and final residence, and undergo a range of mineralogical changes. These changes are principally due to the ingress of hydrous fluids present at shallower depths, causing hydration. The interaction with hydrous fluids rarely happens as a single-stage alteration process and rocks may contain mineral assemblages reflecting partial equilibration at several temperatures, pressures, and fluid compositions.

There is no internationally accepted classification of altered ultramafic rocks or indeed consistency in the names used. Here we use a scheme that is essentially a variation of Fig. 1, but with the anhydrous minerals replaced by their commonest hydrous equivalents: serpentine ($Mg_3Si_2O_5(OH)_4$), tremolite ($Mg_5Ca_2Si_8O_{22}(OH)_2$), and talc ($Mg_3Si_4O_{10}(OH)_2$).

In nature, rocks at the surface are rarely free from any hydration, and indeed rocks that are totally hydrated are common. However, many occurrences fall between these extremes. This continuum of compositions is shown graphically in Fig. 3 to demonstrate the wide range of possible mineralogical mixtures in naturally occurring ultramafic rocks.

The compositional space of ultramafic rocks forms a prism, but trying to plot and compare compositions is difficult in a 3D space. However, it is inferred from previous studies of mineral carbonation[2,13] and from results reported here that (i) orthopyroxene and clinopyroxene behave similarly, but are significantly inferior to olivine in terms of CO_2 mineralization potential and that (ii) various types of amphiboles also behave similarly, but are inferior to serpentine. The compositional prism can then be simplified to a vertical section through the apex to give a simple plot most relevant to a CCSM application (Fig. 3).

The vertical section can then be divided in to composition classification fields (Fig. 4) and used to compare rocks of various types. The plot of compositions is based on the volume proportions of constituent minerals as shown in black and this is closely allied to the degree of hydration as shown in red. This diagram emphasizes the continuum of compositions that can be seen in a simple graphical form. Following

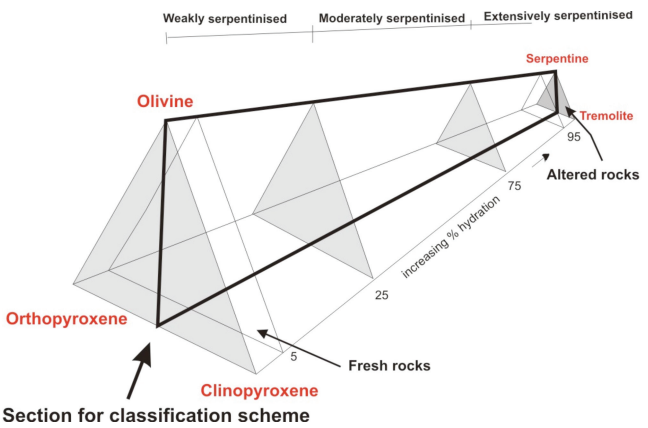

Figure 3. The range of mineralogical compositions of naturally occurring ultramafic rocks, showing the plane through the apex used for classification.

| *Greenhouse Gas Sci Technol.* **4**:440–451 (2014); DOI: 10.1002/ghg

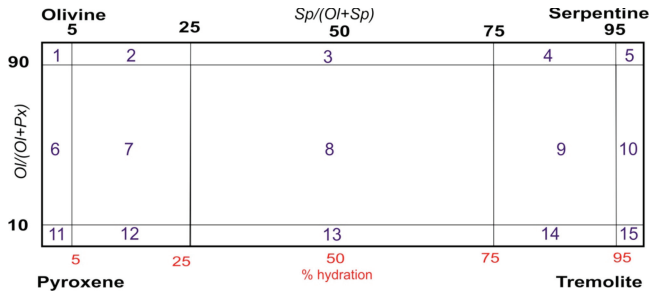

Figure 4. A classification diagram for ultramafic rocks based on the proportions of constituent minerals.

from the information in Figs 1 and 2, compositions at the top of the diagram have higher Mg contents and those at the bottom more Si and less Mg and therefore are less useful for CCSM on the basis of initial composition.

The nature of ultramafic rocks is complex and most natural occurrences, large enough to be a resource for CCSM, will be variable and inhomogeneous and this will have an effect on their use as a source material. They will consist of a mixture of the anhydrous primary minerals and secondary hydrous minerals.

Global distribution of ultramafic rocks

The various types of ultramafic rocks are not uniformly distributed around the world and certain types of geological bodies and mineral combinations are far more abundant than others. An estimate of these global proportions has been made using information from previous national studies[15–18] and data from published datasets.[19–22] From these data we have made a rough estimate of the volumes of the various types of geological bodies and the proportions of constituent minerals. The total resource is around 90 terra tones (sufficient to capture global emissions for 500 years), detail of the analysis will be the subject of a separate publication and a summary is shown graphically in Fig. 5. The detail of the type of geological body is not of importance to this aspect of the study, only the proportions of the constituent minerals and their relative abundance. These data show that serpentine and serpentine-olivine mixtures are volumetrically dominant on a global scale.

Laboratory testing of ultramafic rocks

A range of rock types and minerals has been tested in the laboratory for their suitability for use in mineral carbonation.[7,8,10,13,23–31] A range of techniques to accelerate the liberation of Mg, including acid leaching, heat treatment and very fine grinding was used. In addition, for each technique a range of parameters such as acid concentration, temperature, pressure etc. have been tested. This makes comparison of the data difficult and estimation of the Mg extraction potential of different types of rocks impossible. Of particular importance is the behavior of serpentine, as the previous section shows, it is the main constituent of the most abundant potential source rocks. Serpentine occurs as two main types, lizardite and antigorite, with in some cases, chrysotile as a minor constituent. Serpentinite samples have been tested by

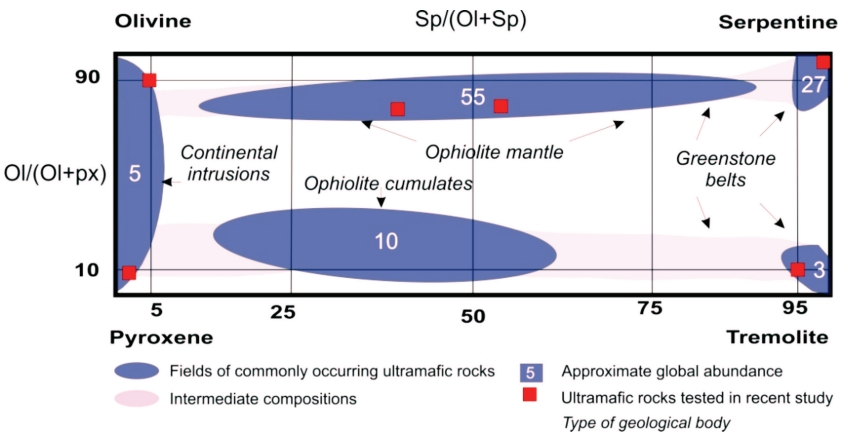

Figure 5. The range of compositions of ultramafic rocks and an indication of the proportion (area %) of the global abundance and the composition of the main rock types tested.

various workers, but the relative potential for Mg extraction of the two main types is unclear. Some experiments show that antigorite is much better than lizardite,[13] while others suggest that lizardite is similar or better.[30] This is an important point that needs clarification as lizardite is the most abundant on a global scale.

Experimental program

The preceding sections have described the classification and wide range of compositions of ultramafic rocks. However, prior to our investigation, experimental studies of mineral carbonation have largely concentrated on the simple olivine-rich or serpentine-rich end-members and the vast majority of ultramafic rock compositions were untested.[4,10,13,31] Here we emphasize that many ultramafic rocks consist of intimate mixtures of olivine, pyroxene and serpentine as shown in Fig. 5. For the testing program we tried to cover the whole spectrum of compositions using rocks as close as possible to the pure end members, together with intermediate compositions likely to be the largest potential source rocks on a global scale. Over 30 rocks were actually tested and those discussed in detail here are listed in Table 1 and shown in Fig. 5.

The experiments described here were carried out to examine the efficiency of Mg extraction by acid leaching using the method described by the authors elsewhere.[7,8,28] The ammonium bisulfate process was selected due to the potential for recycling of the chemicals used in the various steps and the wide interest in such a processes, as discussed in the introduction section. A set of standard conditions was used and the only variable was the composition of the rock tested. Each sample was crushed and milled to a grain size of 75–150 μm, this means that there should not be a large variation in the total surface area of particles. 1.4M ammonium bisulphate was used as leaching agent, a temperature of 100 °C, 1bar pressure and a solid/liquid ratio of 50g/l were used throughout. A three neck flask glass reactor was used with a constant stirring rate of 800 rpm and heating using a silicon bath. A condensation apparatus was connected to the flask to prevent vapor loss of NH_3.

The starting chemical composition of the rock was determined by X-ray fluorescence analysis (XRF) at the Panalytical Laboratory at BGS and the results are given in Table 2. Mg extraction from the mineral lattice was quantified (wt%) using a Thermo-Fisher Scientific X Series Inductively Couple Plasma-Mass Spectrometer (ICP-MS). For the analysis, 1 mL of sample was acidified with 2 mL of HNO_3 and then diluted to 100 mL with deionized water. For

Table 1. List of samples.

Rock type	Location	Sample No.
Olivine rock	Norway (Minelco)	ET 23
Lizardite serpentinite	Ballantrae, Ayrshire, Scotland	ET 1
Antigorite serpentinite	Col del Lis, Lanzo Massif, Italy	ET 29
Antigorite serpentinite	Cedar Hills, Pennsylvania, USA	ET 30
Clinopyroxenite	Khor Fakkan, UAE	ET 27
Amphibole rock	Dadna, UAE	ET 28
Harzburgite	Masafi, UAE	ET 25
Harzburgite	Ismah, UAE	ET 26

Table 2. Bulk composition of major elements determined by XRF.

	$Si0_2$	MgO	$A1_2O_3$	Fe_2O_3t	Mn_3O_4	CaO	Cr_2O_3	NiO	LOI	Total
ET1	37.70	38.56	1.40	7.48	0.13	0.03	0.36	0.26	14.40	100.32
ET23	41.88	48.07	0.38	7.69	0.11	0.42	0.48	0.36	0.77	100.16
ET25	40.51	38.39	1.91	8.50	0.14	3.02	0.37	0.28	7.82	100.94
ET26	40.92	37.91	0.96	8.24	0.14	1.68	0.55	0.27	10.06	100.73
ET27	49.33	20.63	4.53	6.29	0.14	17.22	0.28	0.03	1.12	99.57
ET28	45.86	12.11	12.96	9.34	0.19	14.94	0.14	0.02	3.73	99.29
ET29	39.88	36.22	2.41	8.36	0.14	0.41	0.39	0.29	11.25	99.35
ET30	39.68	38.80	1.16	7.24	0.09	0.49	0.37	0.29	12.30	100.42

Weight% oxide. Trace components not listed.

instrument calibration, scandium (100 μg/L), rhodium (20 μg/L) and iridium (10 μg/L) in 2% trace analysis grade (Fisher Scientific, TAG, Loughborough, UK) HNO_3 were used as internal standards. Also for calibration, external standards for elements were prepared in the range 0–100 μg/L (ppb). An autosampler (Cetac ASX-520) and a concentric glass venture nebulizer (ThermoFisher Scientific, Loughborough, UK) were used and the data processing was undertaken using a Plasmalab software (version 2.5.4, Thermo-Fisher Scientific, Loughborough, UK). Analysis has been carried out in triplicate.

For some compositions, a single sample was tested. However, to define the reactivity of serpentine we tested several samples to clarify the confusion about which type has better leaching properties.

All samples used have been subjected to a detailed geological characterization that included examination of hand specimens, study of thin sections by optical, petrographic microscope and analysis of pre- and post-experimental material by scanning electron microscope (SEM). Bulk mineralogy was determined by X-ray diffraction (XRD) using a PANalytical X'Pert Pro series diffractometer equipped with a cobalt-target tube, X'Celerator detector and operated at 45kV and 40mA. The samples were scanned from 5 to 85°2θ at 0.33°2θ/min. Diffraction data were initially analyzed using PANalytical X'Pert Highscore Plus version 2.2a software coupled to the latest version of the International Centre for Diffraction Data (ICDD) database.

Following identification of the mineral species present in the sample, mineral quantification was achieved using the Rietveld refinement technique[32] also using the PANalytical X'Pert Highscore Plus version 2.2a software.

The SEM analysis was performed using a LEO 435VP variable pressure digital scanning electron microscope. The SEM instrument was equipped with a KE Developments four-quadrant (4 diode-type) solid-state detector for backscattered electron imaging (BSEM). Mineral identification was aided by qualitative observation of energy-dispersive X-ray spectra recorded simultaneously during SEM observation, using an Oxford Instruments INCA energy-dispersive X-ray microanalysis (EDXA) system. Description of textural and mineralogical characteristics observed in the thin sections was completed using a Zeiss Axioplan 2ie optical microscope, with digital photomicrographs captured using a Zeiss Axiocam MRc5 camera.

Table 3. The bulk mineralogy of samples tested determined by XRD.

Rock type	Sample No.	Lizardite 1T	Chrysotile	Antigorite	Forsterite	Ortho-pyroxene	Clino-pyroxene	Amphibole Tremolite	Clinochlore	Montmorillonite	Quartz	Anorthite	Prehnite	Epidote	Dolomite
olivine rack	ET23	1.3			84.2	6.4		3	3.2		0.2				
lizardite serpentinite	ET1	92.3	7.5												
antigorite serpentinite	ET29			93.8					4.2						
antigorite serpentinite	ET30A	2.9		85.3	5.2					4.2	2.4	1.3			
antigorite serpentinite	ET30B	14.3		73.3	38.3					3.2	2	1.8			
clinopyroxenite	ET27	3.4			10.9	6.4	72.7	1.1				5.5			
amphibole rock	ET28							58.9	10.2		0.2		27	3.7	
harzburgite	ET25	56.5	2.1		26.1	7.6	4.7	0.7							2.3
harzburgite	ET26	63.4	3.4		12.3	15.4	4.2	0.9							0.3

Trace components not listed

The composition of the samples is best illustrated by the mineralogy determined by quantitative powder XRD (PXRD) and the results are given in Table 3. Accurate identification and quantification of serpentinites using Rietveld refinement of PXRD data is however difficult. This is mainly due to strong superposition of the main diffraction peaks[33] that originate from the different polymorphs of the serpentine minerals that constitute the rock. In addition, a straightforward application of the Rietveld method to poorly crystalline mixtures containing disordered phases such as chrysotile is not possible.[34] Therefore, to ensure the accuracy of the results presented in this paper, the phase concentrations obtained from PXRD quantitative analysis have been cross-checked with the results of modal analysis performed using optical microscopy and the loss of ignition measured alongside XRF analysis. In addition a few qualitative FTIR analyses were undertaken, mainly to confirm the presence of chrysotile. Nevertheless, the quantitative analysis of samples containing both lizardite and chrysotile could still have some inaccuracy.

Due to difficulty in getting a pure amphibole rock within the time available a sample that showed to contain prehnite, an alteration mineral similar to anorthite feldspar, was used.

Particular attention was paid to the types of serpentine. For lizardite serpentinite, a sample collected from Ballantrae, Scotland, was used. This is one of several collected from there and other localities and the results show that all the lizardite samples behave in a similar manner. This sample is therefore regarded as typical and representative of lizardite serpentinite. For antigorite, a very pure sample collected by BGS from Liguria in NW Italy was used as the type sample and is plotted on the following Figs 6, 7, 8. It gave very similar results to antigorite serpentinites from Shetland, UK and is therefore thought to be representative.

A sample from Cedar Hills, USA that was originally used by the Albany Research Center ARC laboratories[13] was also examined. The Cedar Hills sample has been supplied by ARC as a 'standard antigorite rock' and used in various laboratories for experiments.[13,24,30] Tests and experiments were carried out on this rock. Two samples were examined by PXRD and gave contrasting results, one showed a high antigorite content (85%) with a little lizardite, while the other showed less antigorite (73%) but substantial lizardite (14%). Examination by optical microscopy of

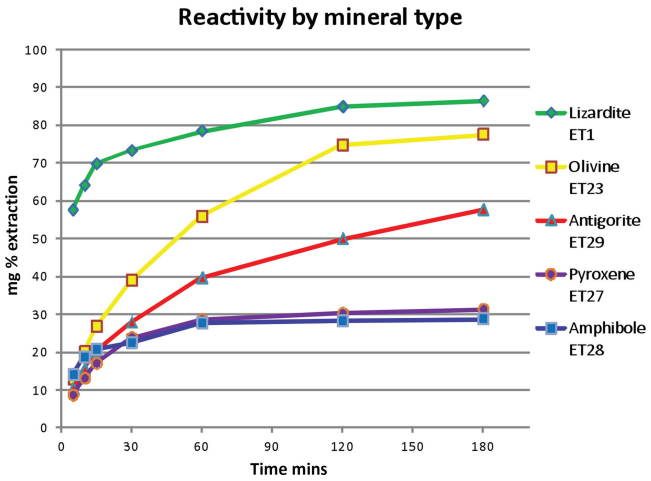

Figure 6. The reactivity of each mineral type as a function of the extraction time using 1.4M ammonium bisulfate. Copyright Energy Technologies Institute.

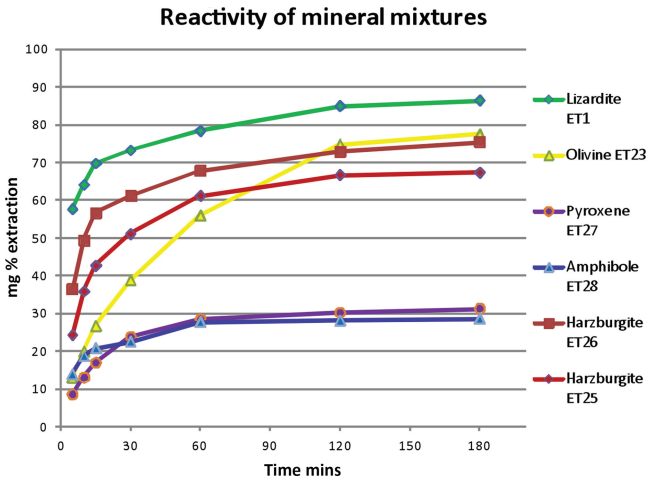

Figure 7. Plot of Mg extraction for rocks of mixed mineral compositions as a function of time. Copyright Energy Technologies Institute.

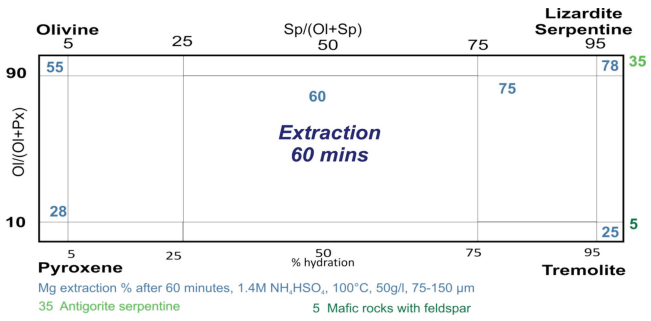

Figure 8. Extraction efficiencies of the tested ultramafic rocks in terms of composition—Reaction time 60 min. Copyright Energy Technologies Institute.

small (few mm), rock fragments from the same sample as used for experiments, showed a range of different rock types. It contained antigorite serpentinite, fragments of lizardite serpentinite with olivine relicts, partially altered to antigorite and a piece of microgabbro, a mafic rock consisting dominantly of feldspar and partially altered clinopyroxene. These fragments would account for the lizardite, anorthite feldspar, quartz and clay reported by PXRD. There is clearly the possibility of significant variation in the proportions of these rocks in a material being used as 'standard' antigorite serpentinite. This could partly explain the variation between results reported previously and emphasizes the necessity of expert geological advice during sample collection and characterization before experiments are carried out.

Experimental results

The full experimental methodology has been described elsewhere.[7,8] The data of importance to this paper are the results of the Mg extraction (expressed as the wt%, measured by the proportion in the leached liquid compared to the content in the starting rock powder), with increasing time using standard conditions. The data are plotted in Fig. 6 and for simplicity the dominant mineral is referred to, rather than the rock name. This shows that lizardite has the best properties with a large amount of Mg extracted in a very short time (nearly 80% after 1 h, and nearly 90% after 3 h). Olivine also shows a high total extraction, nearly 80%, but the short-term extraction rate is much lower with only 55% Mg extracted after 1 h. The data show that antigorite exhibits a much lower extraction than lizardite, with total extraction less than 60% and only 35% after 1 h.

Pyroxene and amphibole-rich rocks have very similar properties, with a total extraction around 30% but little increase after 1 h. This early release possibly reflects Mg from the minor constituents of these rocks such as serpentine and suggest that the pure minerals probably release little Mg and have a low total extraction.

The data shown here for the end-member compositions can essentially be used in a predictive way to estimate the reactivity of any combination of these minerals. This is demonstrated by the results from samples with mixed mineral compositions shown in Fig. 7. The harzburgites, that are a mixture of serpentine and olivine with minor pyroxene, show extraction intermediate between the two main constituents at 1 h, but the low extraction from pyroxene means that after 3 h they are worse than pure olivine.

The extraction efficiencies of the range of rocks tested are shown on the classification rectangle (Fig. 8). It is possible that an extraction time around 60 min might be appropriate for an industrial process considering the large volumes to be treated in unit time and capital costs, and hence this is shown in Fig. 8.

This plot shows clearly that, considering a 60-min leach time, rocks rich in lizardite serpentine release the most Mg. The extraction efficiency decreases significantly as the proportion of olivine increases. As the proportion of antigorite serpentine or particularly pyroxene and amphibole increases the extraction falls to efficiencies less than 50% and is probably unacceptable. The extraction efficiency of most ultramafic rocks can be predicted, if the mineral proportions are known, by interpolation of the values shown on the diagram.

Reaction residues

A detailed mineralogical study of the starting materials and the reaction residues provides important information about the processes that are taking place during the reactions and enables suggestions to be made about the mechanisms involved in Mg leaching.

Examination of the starting material and the residues from leaching (3 h) lizardite serpentine shows little change in the appearance of the particles (Fig. 9); some of the smallest particles may have dissolved but the larger particles retain their starting morphology. This demonstrates that almost all the Mg ions can be removed but the particles are not reduced to powder and remain much the same size and shape as before leaching. Microanalysis shows that the particles now consist solely of silica, and XRD reports that this is amorphous. Serpentine has a layered structure consisting of polymerized silicon-oxygen layers separated by Mg and hydroxyl layers. It appears that the acid very effectively penetrates the crystals along the Mg interlayers and removes it. During this process the regular arrangement of the silicate sheets is disrupted resulting in the amorphous character but the physical integrity of the particle remains almost intact. This is in agreement with the observations of Schott *et al.*,[35] who reported that during leaching of serpentine minerals the abundant Mg cations are selectively removed from the mineral lattice leaving behind silica that undergoes important polymerization of silica tetrahedra.

The leaching residuum also contains small amounts of leach-resistant minerals from the starting material,

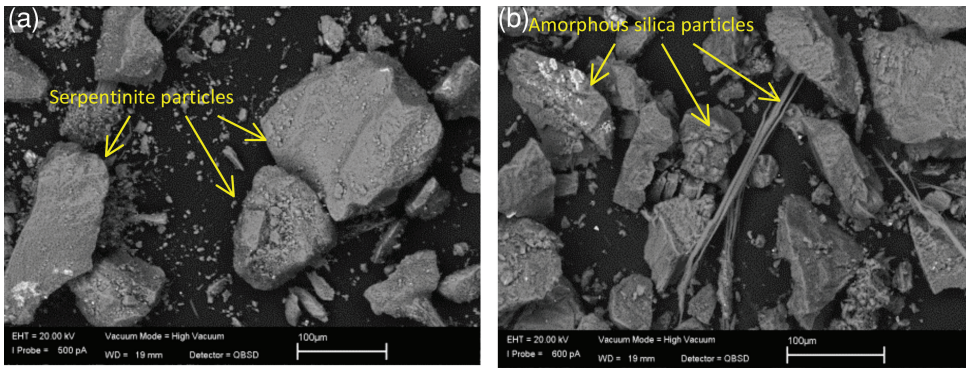

Figure 9. BSE photomicrographs of serpentinite rock powder before (a) and after (b) acid leaching of Mg ions. The Mg-rich silicate is transformed into silica-rich particles retaining the morphology of the original material.

i.e. magnetite/chromite, pyroxene, chlorite and amphibole. In addition, up to 12% of newly formed ammonium, magnesium sulfate hexahydrate (boussingaultite) and to lesser extent other Mg sulfate hydrate species have been observed during SEM examination and have been confirmed by PXRD. These minerals occur as either efflorescent precipitates on particles or aggregates with other solids present in the residuum. They are a by-product of the leaching process and formed from the solution by a reaction between experimental fluids (ammonium bisulfate) and extracted magnesium.

The olivine test sample was supplied by Minelco, an industrial minerals company, and consisted of clean (small amount of fines) angular, roughly equidimensional particles predominantly of olivine (ca 85%), with minor amounts of pyroxene, chlorite, serpentine, talc, amphibole, and traces of quartz.

Olivine belongs to a group of ortho-silicates that contain isolated silicon-oxygen tetrahedra linked by (Mg, Fe) atoms. This 'isolated' structure should, in theory, promote easier leaching of cations;[4] however, our experimental results show that the leaching efficiency of olivine is lower than that of serpentine under the given conditions (Fig. 7). This is possibly related to the amount of secondary boussingaultite formed from the leachate solution. Although leachate samples were taken before the solution had cooled, it is possible that some of the Mg leached from the olivine crystal structure had already been locked up as boussingaltite and reduced the total amount of Mg released, as measured in the leachate solution. The features observed in the post-experimental residue are very different to those in the starting material, the large olivine particles (75–150 μm) have generally disintegrated to smaller fragments of amorphous silica intergrown with boussingaultite. These also occur as scattered, large, up to 700 μm, angular, aggregates. A few euhedral crystals of pyroxene, chlorite and chromite, identified by micro-analysis, showed minimal change (Fig. 10).

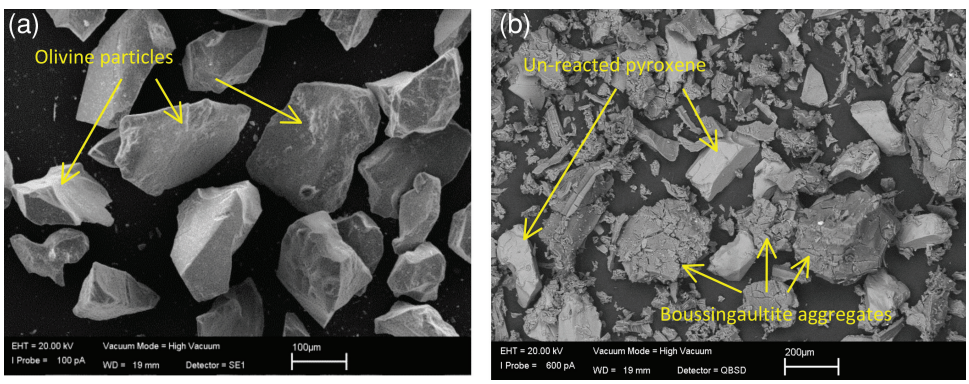

Figure 10. BSE photomicrographs of olivine rock powder before (a) and after (b) acid leaching of Mg ions.

Discussion

A set of Mg extraction experiments has been carried out, under identical experimental conditions, using an ammonium bisulfate solution. This is the first time a series of consistent leaching experiments have been carried out on a wide range of compositions of well-characterized ultramafic rocks where the only variable was the type of rock. This is a significant step forward in the recognition of the importance of the influence of feed material on the suitability of various types of ultramafic rocks for CCSM and enables the leaching behavior of many types of ultramafic rocks to be predicted. These results are probably applicable to other acid leach treatments since the removal of metals from the silicate structure is a metal to proton exchange reaction and directly depends on pH. They may not be applicable to other Mg extraction methods.

The behavior of different minerals during acid leaching and other extraction methods is related to the crystal structure and the variation in the type and strength of the bonds that hold the Mg ions in the silicate structure. During the dissolution of a multi-oxide mineral the rate-limiting step is the break-up of the metal-oxygen bond essential to maintain the mineral structure.[36] The removal of metals from the silicate structure occurs through a metal to proton exchange reaction, as demonstrated in previous work by Schott *et al.*[35] and therefore it depends strongly on pH. According to Schott *et al.*,[35] in general, under acidic conditions, monovalent metal-oxygen bonds break more rapidly than divalent metal-oxygen bonds, which in turn break faster than trivalent bonds. Si-O bonds[35] are the slowest to be broken and this mostly involves H_2O adsorption rather than a Si for H ion exchange reaction.[37] This can explain why some minerals rich in silica or with other less leachable cations in their lattice (e.g. Al) are difficult to dissolve.

The experimental study involved two types of serpentine mineral that possess a different crystal structure. Whereas lizardite consists of flat layers of silica and magnesia, in antigorite the arrangement of these layers is modulated (wavy) causing the position of atoms to change from zone to zone in the crystal structure. This apparently minor change has an appreciable effect on the cation leaching properties of antigorite as shown on Figs 6, 7, and 8; the amount of Mg extracted is significantly lower for antigorite. The higher resistance of antigorite to leaching can possibly be explained by this structural difference. Antigorite is also considered more thermally stable than lizardite due to more effective inter-layer interactions, such as the inversion of the tetrahedral sheet that creates a three dimensional network of chemical bonds (compared to the two-dimensional network in lizardite) that results in a sort of 'chemical cement'.[38]

Conclusions

There are large global resources of ultramafic rocks with potential to play a significant role in CO_2 sequestration by mineralization if technology can be developed to make the process energetically and economically viable. Ultramafic rocks are a family of complex, variable rocks and this is described here to help technologists and engineers understand the range of problems that need to be addressed to adapt or develop processes to deal with the different types of rock resources.

A set of Mg leaching experiments have been carried out using ammonium bisulphate, under constant conditions, to investigate the variation in leaching properties of the full range of ultramafic rocks compositions. From testing the Mg extraction over a 60-min period the conclusions are:

1. Lizardite serpentinites, with ca 80% extraction, are the most suitable feed material for aqueous leaching with ammonium bisulphate.
2. Olivine gives reasonable results, 55% extraction.
3. Serpentinized peridotites, a mixture of olivine and lizardite with some pyroxene (probably the largest resource worldwide), give results between these extremes with typically 65% extraction.
4. Antigorite serpentinites are poor, 40% extraction.
5. Rocks rich in amphibole and pyroxene are poor, typically 25% extraction.
6. Rocks rich in antigorite, pyroxene and amphibole should no longer be considered as suitable resources for utilization by indirect mineral carbonation methods using acid leaching of Mg cations.

The development of processes that give good extraction from mixtures of serpentine and olivine is important to enable use of the commonest type of feedstock resource. The release of Mg from olivine is much greater after 3 h; therefore the utilization of mixed rocks might require longer leaching times to maximize efficiency.

The choice of feedstock material can have a huge impact on the amount of Mg cations released for carbonation and accurate characterization of

resources and awareness of the consequences are vital to development of processes and any planning for future deployment.

Acknowledgments

We thank the Energy Technologies Institute (ETI) that commissioned and funded the work as part of its CCS program. Doris Wagner (BGS) is thanked for carrying out the XRD analysis. Project partners from Caterpillar and the Centre for Process Innovation contributed valuable discussion during the project. The financial support of the Centre for Innovation in Carbon Capture and Storage (CICCS) through the Engineering and Physical Sciences Research Council, EPSRC (EP/F012098/2) is gratefully acknowledged. MTS, AML, and JN publish with permission of the Executive Director of the British Geological Survey (NERC).

References

1. IPCC, Summary for policymakers, in *IPCC Special Report on Renewable Energy Sources and Climate Change Mitigation,* ed by Edenhofer O, Pichs-Madruga R, Sokona Y, Seyboth K, Matschoss P, Kadner S *et al.* Cambridge University Press, Cambridge, UK and New York, NY, USA (2011).
2. Goff F and Lackner KS, Carbon dioxide sequestering using ultramafic rocks. *Environ Geosci* **5**:89–101 (1998).
3. Sanna A, Hall MR and Maroto-Valer MM, A review of post-processing pathways in carbon capture and storage by mineralization. *Energ Environ Sci* **5**:7781–7796 (2012).
4. Gerdemann SJ, O'Connor WK, Dahlin DC, Penner LR and Rush H, Ex situ aqueous mineral carbonation. *Environ Sci Technol* **41**:2587–2593 (2007).
5. Béarat H, McKelvy MJ, Chizmeshya AVG, Sharma R and Carpenter RW, Magnesium hydroxide dehydroxylation/carbonation reaction processes: Implications for carbon dioxide mineral sequestration. *J Am Ceram Soc* **85**:742–748 (2002).
6. Chizmeshya AVG, McKelvy MJ, Squires K, Carpenter RW and Bearat H, *A Novel Approach To Mineral Carbonation: Enhancing Carbonation While Avoiding Mineral Pretreatment Process Cost*, NETL, DOE, Oak Ridge, TN, USA (2007). DOI:10.2172/924162
7. Wang X and Maroto-Valer M, Dissolution of serpentine using recyclable ammonium salts for CO_2 mineral carbonation. *Fuel* **90**:1229–1237 (2011).
8. Wang X and Maroto-Valer M, Integration of CO_2 capture and mineral carbonation by using recyclable ammonium salts. *Chem Sus Chem* **4**(9):1291–1300 (2011).
9. Kodama S, Nishimoto T, Yamamoto N, Yogo K and Yamada K, Development of a new pH-swing CO_2 mineralization process with a recyclable reaction solution. *Energy* **33**:776–784 (2008).
10. Park AHA and Fan LS, CO_2 mineral sequestration: Physically activated dissolution of serpentine and pH swing process. *Chem Eng Sci* **59**:5241–5247 (2004).
11. Eloneva S, Said A, Fogelholm KJ and Zevenhoven R, Preliminary assessment of a method utilizing carbon dioxide and steelmaking slags to produce precipitated calcium carbonate. *Appl Energ* **90:**329–334 (2012).
12. Lackner KS, Wendt CH, Butt DP, Joyce EL Jr and Sharp DH, Carbon dioxide disposal in carbonate minerals. *Energy* **20**:1153–1170 (1995).
13. O'Connor WK, Dahlin DC, Rush GE, Gerdemann SJ, Penner LR and Nilsen DN, *Aqueous Mineral Carbonation: Mineral Availability, Pre-treatment, Reaction Parametrics and Process Studies,* DOE/ARC –TR-04-002. Albany Research Center, Albany, USA (2005).
14. Gillespie MR and Styles MT, *BGS Rock Classification Scheme: Volume 1. Classification of Igneous Rocks*, Report, RR 99-06. British Geological Survey, Nottingham, UK (1999).
15. Voormeij DA and Simandl GJ, *Ultramafic rocks in British Columbia: Delineating Targets for Mineral Sequestration of CO_2.* British Columbia Ministry of Energy, Mines and Petroleum Resources, Victoria, British Columbia, Canada, pp 157–167 (2004).
16. Krevor SC, Graves CR, Van Gosen B and McCafferty A, *Mapping the Mineral Resource Base for Mineral Carbon-Dioxide Sequestration in the Conterminous United States.* [Online]. U.S. Geological Survey Digital Data Series 414 (2009). Available at: http://pubs.usgs.gov/ds/414 [21 January 2014].
17. Bailly L, *Séquestration Minérale Ex-Situ du CO_2 : Inventaire Français des Roches Basiques et Ultrabasiques*, Bureau de Recherches Géologiques et Minières (BRGM), Orleans, France (2004).
18. Mani D, Nirmal Charan S and Kumar B, Assessment of carbon dioxide sequestration potential of ultramafic rocks in the greenstone belts of southern India. *Curr Sci India* **94:**53–59 (2008).
19. Natural Resources Canada, *Mineral Deposit Database. Geoscience Data Repository.* [Online]. Geological Survey of Canada, Earth Sciences Sector, Natural Resources Canada, Government of Canada (2012). Available at: http://gdr.nrcan.gc.ca/minres/index_e.php [4 November 2013].
20. Asch K, *The 1:5 million International Geological Map of Europe and Adjacent Areas*. [Online]. BGR (Hannover) (2005). Available at: http://www.bgr.de/karten/igme5000/igme5000.htm [21 January 2014].
21. Exxon Production Research Company and The American Association of Petroleum Geologists, *Tectonic Map of the World 1:10000000*. Exxon Production Research Company, Houston, TX, USA (1985).
22. Commission for the Geological Map of the World, *Geological Map of the World Scale 1:25 000 000, 2nd edition*. CGMW-UNESCO, Paris, France (2000).
23. Carey WJ, Ziock HJ and Guthrie DG Jr, Reactivity of serpentine in CO_2-bearing solutions: Application to CO_2 sequestration. *Am Chem Soc Div Fuel Chem* **49**(1):371–372 (2004).
24. Alexander G, Maroto-Valer M and Gafarova-Aksoy P, Evaluation of reaction variables in the dissolution of serpentine for mineral carbonation. *Fuel Sci* **86**:273–281 (2007).
25. Hänchen M, Prigiobbe V, Storti G, Seward TM and Mazzotti M, Dissolution kinetics of fosteritic olivine at 90–150° C including effects of the presence of CO_2, *Geochim Cosmochim Ac* **70**:4403–4416 (2006).
26. Teir S, Eloneva S, Fogelholm CJ and Zevenhoven R, Fixation of carbon dioxide by producing hydromagnesite from serpentinite. *Appl Energ* **86:**214–218 (2008).

27. Krevor S and Lackner K, Enhancing serpentine dissolution kinetics for mineral carbon dioxide sequestration. *Int J Greenhouse Gas Control* **5**(4):1073–1080 (2011).
28. Sanna A, Dri M, Wang X, Hall MR and Maroto-Valer MM, Carbon dioxide capture and storage by pH swing aqueous mineralisation using a mixture of ammonium salts and antigorite source. *Fuel* **114**:153–161 (2013).
29. Olsson J, Bovet N, Makovicky E, Bechgaard K, Balogh Z and Stipp SLS, Olivine reactivity with CO_2 and H_2O on a microscale: Implications for carbon sequestration. *Geochim Cosmochim Ac* **77:**86–97 (2012).
30. Gerdemann SJ, Dahlin DC, O'Connor WK and Penner LR, *Carbon Dioxide Sequestration by Aqueous Mineral Carbonation of Magnesium Silicate Minerals.* DOE/ARC, Albany, New York, USA (2003).
31. Tier S, Kuusik R, Fogelholm CJ and Zevenhoven R, Production of magnesium carbonates from serpentinite for long-term storage of CO_2. *Int J Miner Process* **85:**1–15 (2007).
32. Snyder RL and Bish DL, Quantitative analysis, in *Modern Powder Diffraction, Reviews in Mineralogy*, ed by Bish DL and Post JE, Mineralogical Society of America, Washington, DC, USA, pp. 101–144 (1989).
33. Cavallo A and Rimoldi B, Chrysotile asbestos in serpentinite quarries: A case study in Valmalenco, Central Alps, Northern Italy. *Environ Sci Process Impacts* **15(7)**:1341–1350 (2013).
34. Gualtieri AF and Artioli G, Quantitative determination of chrysotile asbestos in bulk materials by combined Rietveld and RIR methods. *Powder Diffr* **10(4)**:269–277 (1995).
35. Schott J, Pokrovsky OS and Oelkers EH, The link between mineral dissolution/precipitation kinetics and solution chemistry. *Rev Mineral Geochem* **70:**207–258 (2009).
36. Oelkers EH, General description of multi-oxide silicate mineral and glass dissolution *Geochim Cosmochim Ac* **65:**3703–3719 (2001).
37. Dove PM and Crerar DA, Kinetics of quartz dissolution in electrolyte solutions using a hydrothermal mixed flow reactor. *Geochim Cosmochim Ac* **54:**955–969 (1990).
38. Capitani G and Mellini M, The modulated crystal structure of antigorite: The m=17 polysome. *Am Mineral* **89:**147–158 (2004).

Mike Styles

Mike Styles is a geologist at the British Geological Survey with 35 years of research experience in many fields and an expert on ultramafic rocks. Over the last eight years he has applied this to studies of mineral carbonation in collaboration with chemical engineers.

Aimaro Sanna

Aimaro Sanna did his PhD in Environmental Engineering at Nottingham University studying catalytic processes toward the conversion of biomass in biofuels and biochemicals. He is currently working on clean fossil fuel technologies at Heriot-Watt University with interests in biofuels, heterogeneous catalysis, and carbon capture and storage technologies.

Alicja Lacinska

Alicja Lacinska is a mineralogist/petrologist at the British Geological Survey with several years of experience working on carbon capture and storage by mineralization of ultramafic rocks and serpentinites.

Jon Naden

Jon Naden is an economic geologist at the British Geological Survey with over 20 years of research experience in understanding natural hydrothermal activity and the minerals resources that result from these processes. Recently he has applied this knowledge to studies of natural mineral carbonation.

M. Mercedes Maroto-Valer

Prof. M. Mercedes Maroto-Valer is the Robert Buchan Chair in Sustainable Energy Engineering at Heriot-Watt University. She is the Head of the Institute for Mechanical, Processing and Energy Engineering and leads the pan-University Energy Academy. She has established an international research reputation at the interface between energy and the environment.

